

## EFFECT OF ER DOPING INTO BATIO<sub>3</sub> THIN FILMS: A NANO-STRUCTURAL STUDY

Ooi ZV, Saif AA\* and Poopalan P

School of Microelectronic Engineering,  
University Malaysia Perlis (UniMAP), Pauh Putra Campus,  
02600 Arau, Perlis, Malaysia.

*Sol-gel barium titanate (BaTiO<sub>3</sub>) and erbium doped barium titanate (Er-BaTiO<sub>3</sub>) were deposited on SiO<sub>2</sub>/Si substrates. The phase and crystallinity of the thin films were identified using x-ray diffractometer (XRD). The effect of Er dopant into BaTiO<sub>3</sub> thin film on its grain size and surface roughness was studied using atomic force microscope (AFM) in tapping mode. XRD patterns revealed that the films were crystallized with perovskite structure. At the same time, it was shown that introducing Er dopant into BaTiO<sub>3</sub> thin film caused the dominant peak to shift towards higher angle. AFM micrographs indicated that the films had well distributed grains, dense and crack-free surface. In general, substitution of Er dopant into Ba-site reduced the grain sizes and roughness parameter of the BaTiO<sub>3</sub> which was attributed to the smaller ionic radius of Er.*

**Keywords:** Er-BaTiO<sub>3</sub>, Sol-Gel, Atomic Force Microscopy

### INTRODUCTION

Lead-free perovskite structure ferroelectric BaTiO<sub>3</sub> is one of the most common material widely used in the microelectronic and optoelectronic devices due to its excellent dielectric, ferroelectric, electronic and electro-optic properties as well as a great host lattice to accommodate distinct dopants [1-3]. Literature study shows that many different dopants has been introduced to BaTiO<sub>3</sub> for enhancing its microstructural, electrical and optical properties [1,3,4]. Among these, rare-earth oxides erbium (Er) shows excellent optical properties as an additive to BaTiO<sub>3</sub> for enhancing various properties in several applications [1,5,6].

Surface topography investigation is one of the essential characterization steps that provides film surface quality related fundamental information such as specific optical, electrical, chemical, mechanical or tribological properties [7]. To understand the surface behavior of the Er-BaTiO<sub>3</sub> thin films, numerous parameters can be used to evaluate the surface roughness and they are classified

into four groups: amplitude, functional, spatial and hybrid parameter [8]. However, the most important is the amplitude parameters [4].

Limited information have been found on the surface morphology of the Er-BaTiO<sub>3</sub> thin films. V.V. Mitic *et al.* reported that the Er-BaTiO<sub>3</sub> powder, prepared using conventional solid-state procedure, shows an increase of the Er concentration causes a decrease of the grain size [9]. In this work, Er-BaTiO<sub>3</sub> and BaTiO<sub>3</sub> thin films will be prepared by the sol-gel technique, where the BaTiO<sub>3</sub> served as the reference for the study. The grain size and surface roughness of these films will be examined using AFM. However, XRD data will also be employed to study the crystalline structure of the films.

### MATERIALS AND METHODS

#### *Solution Preparation*

Barium acetate, erbium acetate and titanium (IV) isopropoxide were chosen as the precursors. Acetic acid was used as the

---

\* Corresponding author: Tel: +6 014 247 0306

E-mail: alaeddinsaif@gmail.com

solvent for acetates and 2-methoxyethanol was employed to dissolve the titanium (IV) isopropoxide. A specific amount of barium acetate and erbium acetate was dissolved in the 15 ml of heated acetic acid to form Ba-Er solution and stirred for 120°C until it became clear. This solution was then refluxed at 120°C for 2 hours. Meanwhile, Ti solution was prepared by adding stoichiometric amount of titanium (IV) isopropoxide to 5 ml of 2-methoxyethanol and stirred in room condition. Both solutions were stirred at 500 rpm for 2 hours in the room condition and refluxed immediately for 1 hours at 120°C. The filtered and tightly sealed final solution can be kept for approximately three month in the dry environment. Two different solutions with Ba:Er proportions of 1:0 and 0.9:0.1 were prepared, and labeled as BT and EBT90 respectively, where the BT was used as the reference for the doped BaTiO<sub>3</sub>.

### **Sample Preparation**

Spin-coating method was employed to produce Er-BaTiO<sub>3</sub> thin films by depositing the prepared solution on the SiO<sub>2</sub>/Si substrates. The substrates were cleaned using acetone, IPA and DI water before deposition process was started. Upon drying the substrates, the solution was spin-coated on the substrate at 5000 rpm for 20 s. The samples were then baked at 200°C to vaporize the solvent. In order to prepare a multi-layered sample, the spin-coating and baking processes were repeated until desired thickness was achieved. The samples were then pre-baked at 500°C for 15 min to remove the organic substances and annealed at 900°C for 1 hour to form crystalline structure. Multilayered BaTiO<sub>3</sub> and Er-BaTiO<sub>3</sub> thin films were prepared using the same deposition procedure.

The crystallization of the material was identified using x-ray diffractometer (XRD), with a CuK $\alpha$  radiation source ( $\lambda = 1.54 \text{ \AA}$ ), operated at a voltage of 40 KV and a current of 30 mA. The surface morphology of the films were studied using atomic force microscopy (AFM) (SPA400, SII

Nanotechnology Inc.), operated in tapping mode. The design of tapping mode tips allows AFM to produce a clearly superior result and a more reliable data than using contact mode [10]. In this work, the roughness parameters was obtained at the scanning area of 10x10  $\mu\text{m}^2$  while size of grains was obtained at the scanning area of 1x1  $\mu\text{m}^2$ .

## **RESULTS AND DISCUSSION**

### ***X-ray Diffractometer (XRD)***

Crystalline and structural identification are essential characterization steps prior to other characterizations, as it allows confirmation of the crystalline structure and components existing within the samples. XRD is the most common tool that required simple sample preparation and it is non-destructive towards the samples, which in turn allows the same samples to undergo other characterization tests.

The XRD patterns for BaTiO<sub>3</sub> and Er-BaTiO<sub>3</sub> films are illustrated in Fig. 1. The results are matched to JCPDS 05-0626 file. The results indicates that both films are crystallized with tetragonal phase at room temperature. The figure shows that main peak for perovskite structure in BaTiO<sub>3</sub> is crystallized at 31.57° and shifted to higher angle for Er-BaTiO<sub>3</sub> film indicating the replacement of Ba<sup>2+</sup> ions by Er<sup>3+</sup> ions. Other phases such as Ba<sub>2</sub>TiO<sub>4</sub> and TiO<sub>2</sub> also exist within the films which could be attributed to annealing process.

### ***Atomic Force Microscopy (AFM)***

The roughness parameters of a sample are usually extracted from the surface characterizing equipment and they are described using the statistical method. The average roughness ( $R_a$ ) is the arithmetic mean height that calculated along the assessment line/area. Maximum peak to valley height roughness ( $R_i$ ) is the difference between the highest point and lowest point in the evaluated length/area and it describes the

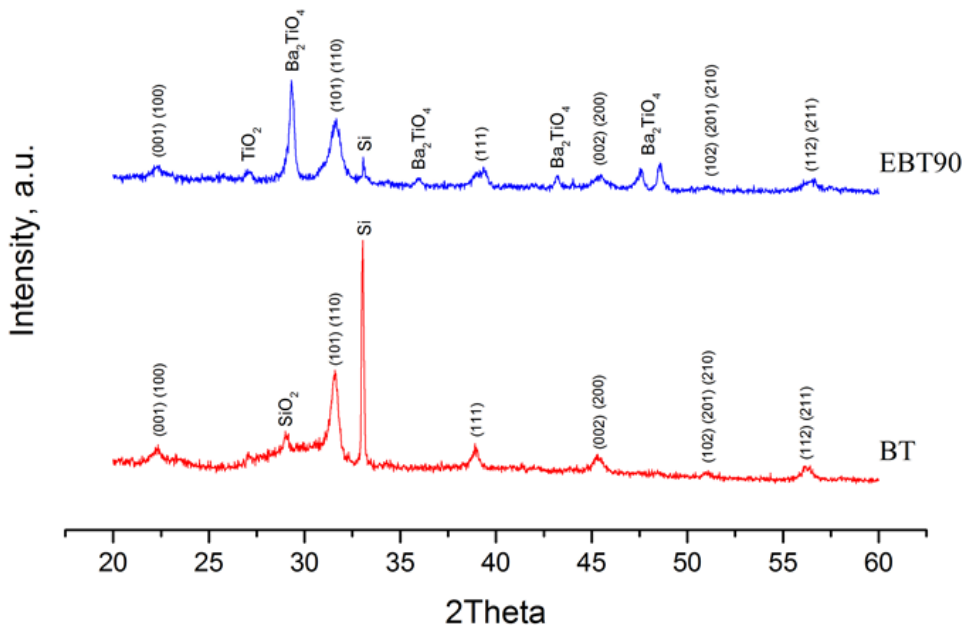


**Fig. 1:** XRD pattern of the BT and EBT90.

overall roughness of the surface. Root mean square roughness ( $R_q$ ) is the square root of the distribution of the surface height, which generally has a greater value than  $R_a$ .  $R_q$  is more sensitive towards the small changes in the profile and it is also used to compute the skew and kurtosis parameters. Skewness roughness ( $R_{sk}$ ) is used to measure the symmetry of the profile about the mean line and it is sensitive to occasional deep valleys or high peak. Roughness kurtosis ( $R_{ku}$ ) is used to describe the sharpness of the probability density of the profile.

Fig. 2 shows the three dimensional AFM micrographs with  $10 \times 10 \mu\text{m}^2$  scanned area for BT and EBT90 films. The obtained images display crack-free and pinhole-free films.

Table 1 shows that the surface roughness values ( $R_a$ ) and RMS roughness values ( $R_q$ ) decrease with the accumulation of Er dopant in BaTiO<sub>3</sub> thin film. Maximum peak to valley height ( $R_t$ ) is considered as an important parameter as it describes the overall roughness of the surface. The results from Table 1 show that the BT is rougher than

EBT90, which indicates that the higher Ba content, the bigger the individual unit cells, leading to larger clumps of grains.  $R_q$  values for all samples are greater than  $R_a$  values, which can be described by the following equation [11].

$$R_a = \frac{1}{L} \int_0^L |y(x)| \cdot dx \quad (1)$$

$$R_q = \sqrt{\frac{1}{L} \int_0^L |y(x)|^2 \cdot dx} \quad (2)$$

where  $L$  is the assessment length along the  $x$ -axis and  $y(x)$  is the variation of the height from assessment line for each data point.

Generally, the negative value of skewness shows the valleys, scratches or pits are dominant along the evaluated area and positive value of skewness indicates the peaks are dominant at scanned surface [7]. For kurtosis,  $R_{ku}$  value below than three indicates a relatively flat surface and called platykurtic (i.e. few high peak and low valleys), while  $R_{ku}$  value above than three indicates a spiky surface and called leptokurtic (i.e. many high peak and low valleys) [11]. Table 1 shows that  $R_{sk}$  values

for both tested samples are positive indicating that peaks are dominant while  $R_{ku}$  values are less than three indicating that the films have a relatively flat surface, which indicates that the solutions are well spread out on the surface during deposition process. Fig. 3 illustrates  $1 \times 1 \mu\text{m}^2$  scanned area of BT and EBT90 films surfaces. The figure shows dense, fine and uniformly distributed grains for both films. The measured grain size as shown in Table 1 decreases upon introduction of  $\text{Er}^{3+}$  dopant into  $\text{BaTiO}_3$ ,

which is due to smaller ionic radius of Er ( $0.96 \text{ \AA}$ ) as compared to Ba ( $1.35 \text{ \AA}$ ). This could indicate that the  $\text{Er}^{3+}$  dopants are substituted into the Ba-site of  $\text{BaTiO}_3$  thin film which in turn creates smaller grains compared to undoped thin film. Introducing  $\text{Er}^{3+}$  ions into  $\text{BaTiO}_3$  lattice alter the nanostructure characteristics which directly affects the electrical and optical properties. This could enable to control the opto-electric parameters by varying the fabrication conditions.

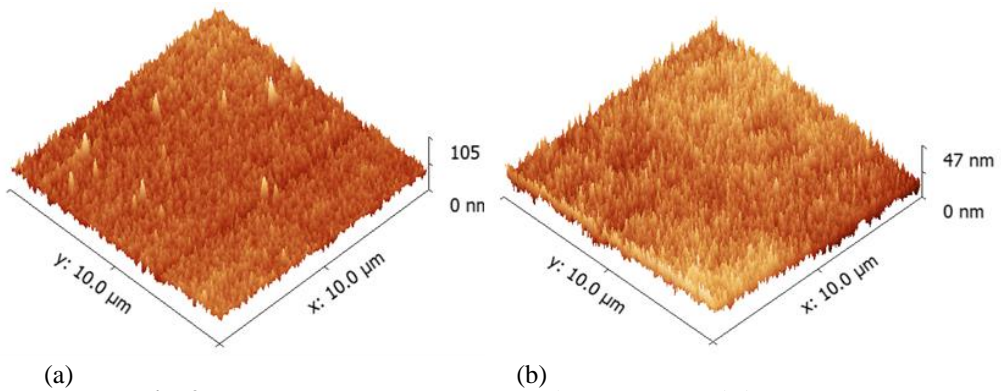


**Fig. 2:** Surface on 3D AFM micrograph for (a) BT and (b) EBT90.

**Table 1:** Roughness parameter of BT and EBT90.

Sample	$R_a$ [nm]	$R_t$ [nm]	$R_q$ [nm]	$R_{sk}$ [nm]	$R_{ku}$ [nm]	Grain Size [nm]
BT	5.623	102.6	7.301	0.176	1.040	78.430
EBT90	3.738	42.8	4.712	0.234	0.188	64.725

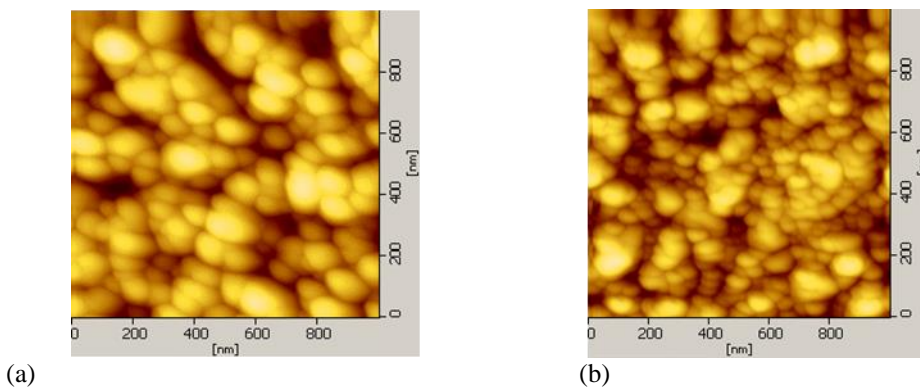


**Fig. 3:** Grain distribution on 2D AFM micrograph for (a) BT and (b) EBT90.

## CONCLUSIONS

BaTiO<sub>3</sub> and Er-BaTiO<sub>3</sub> thin films were fabricated on the SiO<sub>2</sub>/Si substrates using sol-gel technique. The crystallinity and phase identification of both films were performed using x-ray diffractometer (XRD). The surface morphology and grain size were characterized via atomic force microscopy (AFM). The results indicate that crystallized, crack-free Er-BaTiO<sub>3</sub> thin films are efficiently fabricated on SiO<sub>2</sub>/Si substrates by sol-gel technique. The XRD patterns show that the films is crystallized with perovskite structure with a shifting for the dominant peak to higher angle due to the Er dopant substituted in Ba-site of BaTiO<sub>3</sub>. The surface of films show a low surface roughness and relatively small grain size with not more than 100 nm. The smaller ionic radius of the Er occupying the Ba-site causes the reduction of the grain size, which demonstrates the success of the doping process. This shows that it is possible to alter the electrical and optical properties by manipulating the structural parameters of the film which are related to the concentration of Ba:Er.

## REFERENCES

- [1] Chen, L., Wei, X., & Fu, X. (2012). Effect of Er Substituting Sites on Upconversion Luminescence of Er<sup>3+</sup>-Doped BaTiO<sub>3</sub> Films. *Trans. Nonferrous Met. Soc. China*, 22(5) 1156.
- [2] Zhang, Y., Hao, J., Mak, C. L., & Wei, X. (2011). Effect of Site Substitutions and Concentration on Upconversion Luminescence of Er<sup>3+</sup>-Doped Perovskite Titanate. *Opt. Express*, 19(3) 1824.
- [3] Buscaglia, M. T., Buscaglia, V., Viviani, M., Nanni, P., & Hanuskova, M. (2000). Influence of Foreign Ions on The Crystal Structure of BaTiO<sub>3</sub>. *J. Eur. Ceram. Soc.*, 20(12) 1997.
- [4] Teh, Y. C., Saif, A. A., Jamal, Z. A. Z., & Poopalan, P. (2014). Microstructure Study on Gd-doped BaTiO<sub>3</sub> Sol-gel Multilayer Thin Films Using AFM for Optoelectronic. *Adv. Mater. Res.*, 911 251.
- [5] García Hernández, M., Carrillo Romo, F. D. J., García Murillo, A., Jaramillo Viguera, D., Meneses Nava, M. A., Bartolo Pérez, P. & Chadeyron, G. (2010). The Influence of Polyvinylpyrrolidone on Thick and Optical Properties of BaTiO<sub>3</sub>:Er<sup>3+</sup> Thin Films Prepared by Sol-Gel Method. *J. Sol-Gel Sci. Technol.*, 53(2) 246.
- [6] Zhang, H. X., Kam, C. H., Zhou, Y., Han, X. Q., Xiang, Q., Buddhudu, S., Lam, Y. L., & Chan, Y. C. (2000). Photoluminescence at 1.54 μm in Sol-Gel-Derived, Er-Doped BaTiO<sub>3</sub> Films. *J. Alloys Compd.*, 308(1-2) 134.
- [7] Tudose, I. V., Horváth, P., Sucheá, M., Christoulakis, S., Kitsopoulos, T., & Kiriakidis, G. (2007). Correlation of ZnO Thin Film Surface Properties with Conductivity. *Appl. Phys. A*, 89(1) 57.
- [8] Wysocka, K., Ulatowska-Jarza, A., Bauer, J., Holowacz, I., Savu, B., Stanciu, G., & Podbielska, H. (2008). AFM Examination of Sol-Gel Matrices Doped with Photosensitizers. *Optica Applicata*, 38(1) 127.
- [9] Mitic, V. V., Nikolic, Z. S., Pavlovic, V. B., Paunovic, V., Miljkovic, M., Jordovic, B., & Zivkovic, L. (2010). Influence of Rare-Earth Dopants on Barium Titanate Ceramics Microstructure and Corresponding Electrical Properties. *J. Am. Ceram. Soc.*, 93(1) 132.
- [10] Simpson, G. J., Sedin, D. L., & Rowlen, K. L. (1999). Surface Roughness by Contact versus Tapping Mode Atomic Force Microscopy. *Langmuir*, 15(4) 1429.
- [11] Gadelmawla, E. S., Koura, M. M., Maksoud, T. M. A., Elewa, I. M., & Soliman, H. H. (2002). Roughness Parameters. *J. Mater. Process. Technol.*, 123(1) 133.